

MOL #7708

## Functional Interactions Between Nucleotide Binding Domains and LTC<sub>4</sub> Binding Sites of Multidrug Resistance Protein 1 (ABCC1)

LEA PAYEN, MIAN GAO, CHRISTOPHER WESTLAKE, ASHLEY THEIS, SUSAN P.C. COLE and ROGER G. DEELEY

*Division of Cancer Biology and Genetics (L.P., M.G., C.W., A.T., S.P.C.C., R.G.D), Cancer Research Institute, the Department of Biochemistry (C.W.) and the Department of Pathology and Molecular Medicine (A.T., S.P.C.C. R.G.D.), Queen's University, Kingston, Ontario, Canada K7L 3N6*

MOL #7708

# **Running title:**

Catalytic cycle of MRP1

**Corresponding author:** Dr. Roger G. Deeley, Cancer Research Institute, Queen's University,

10 Stuart St., Kingston, Ontario K7L 3N6 Canada. Tel: 613-533-2023; Fax: 613-533-2139;

Email: deeleyr@post.queensu.ca

Number of text pages (including references).....22

Number of figures.....8

Number of tables.....0

Number of references.....42

Number of words:

Abstract..... 249

Introduction.....1,243

Discussion.....1, 478

**ABBREVIATIONS:** MRP, multidrug resistance protein; E<sub>2</sub>17βG, 17β-estradiol-17-β-(D-glucuronide); NBD, nucleotide binding domain; MSD, membrane-spanning domain; CFTR, cystic fibrosis transmembrane conductance regulator; SUR, sulfonylurea receptor; ATP-γ-S, adenosine 5'-O-(thiotriphosphate); AMP-PNP, β,γ-imidoadenosine 5'-triphosphate; AMP-PCP, Adenylylmethylenediphosphate

MOL #7708

## ABSTRACT

MRP1 is a member of the 'C' branch of the ATP-binding cassette (ABC) transporter superfamily. The NH<sub>2</sub>-proximal nucleotide binding domain (NBD1) of MRP1 differs functionally from its COOH-proximal domain (NBD2). NBD1 displays intrinsic high-affinity ATP binding and little ATPase activity. In contrast, ATP binding to NBD2 is strongly dependent on nucleotide binding by NBD1 and NBD2 is more hydrolytically active. Previously, we demonstrated that occupancy of NBD2 by ATP or ADP, markedly decreased substrate binding by MRP1. We have further explored the relationship between nucleotide and substrate binding by examining the effects of various ATP analogs and ADP trapping, as well as mutations in conserved functional elements in the NBDs, on the ability of MRP1 to bind the photoactivatable, high-affinity substrate, leukotriene C<sub>4</sub> (LTC<sub>4</sub>). Overall, the results support a model in which occupancy of both NBD1 and NBD2 by ATP results in formation of a low-affinity conformation of the protein. However, non-hydrolyzable ATP analogs (AMP-PNP and AMP-PCP) failed to substitute for ATP or ATP- $\gamma$ -S in decreasing LTC<sub>4</sub> photolabeling. Furthermore, mutations of the signature sequence in either NBD that had no apparent effect on azido-ATP binding, abrogated formation of a low-affinity substrate binding state in the presence of ATP or ATP- $\gamma$ -S. We suggest that the effect of these mutations, and possibly the failure of some ATP analogs to decrease LTC<sub>4</sub> binding, may be attributable to an inability to elicit a conformational change in the NBDs that involves interactions between the signature sequence and the  $\gamma$ -phosphate of the bound nucleotide.

## Introduction

Multidrug Resistance Protein (MRP) 1 confers resistance to a wide range of natural product cytotoxic agents (Cole et al., 1992; Cole et al., 1994). The protein also transports structurally diverse conjugated organic anions, including the high-affinity physiological substrate, cysteinyl leukotriene C<sub>4</sub> (LTC<sub>4</sub>) (Leier et al., 1994). MRP1 is a member of the 'C' branch of the ATP Binding Cassette (ABC) transporter superfamily. Other 'C' branch members include the cystic fibrosis transmembrane conductance regulator (CFTR), the sulfonyleurea receptors, SUR1 and SUR2, and nine additional MRPs (Dean and Allikmets, 2001).

ABC proteins are generally comprised of two hydrophilic nucleotide-binding domains (NBDs) located at the cytoplasmic surface of the membrane and two functionally linked hydrophobic membrane spanning domains (MSDs), each of which typically has six transmembrane (TM) helices. However, a number of the 'C' branch transporters, including, MRP1, MRP2, MRP3, MRP6 and MRP7, as well SUR1 and SUR2, are unusual in that they have an additional NH<sub>2</sub>-terminal MSD that probably contains five TM helices and has an extracellular NH<sub>2</sub>- terminus (Hipfner et al., 1997; Kast and Gros, 1997). Furthermore, compared with many ABC transporters, the NBDs of the 'C' branch proteins are relatively divergent with some structural features that are characteristic of the ABCC proteins (Cole et al., 1992).

The NBDs of all ABC proteins contain three conserved sequence elements: the Walker A and B motifs and the ABC signature sequence (LSGGQ) or C-motif. The X-ray crystal structures of NBDs of several ABC proteins have made major contributions to understanding the role of these motifs in ATP binding and hydrolysis. For example, the Walker A motif, or P-loop, appears to wrap around the phosphate chain of ATP with the nitrogens of the residues within this motif

MOL #7708

extensively hydrogen bonding with the  $\gamma$ -phosphate of the bound nucleotide, while the Walker B motif contributes an aspartate residue that coordinates and stabilizes a magnesium ion which is indispensable for ATP hydrolysis (Diederichs et al., 2000; Gaudet and Wiley, 2001; Hung et al., 1998). Crystal structures of the soluble ABC protein, Rad50 (Hopfner and Tainer, 2003), and bacterial transporters such as vcMsbA (Chang, 2003) and BtuCD (Locher et al., 2002) indicate that Walker A and Walker B motifs of one NBD cooperate with the C motif of the other NBD, effectively sandwiching nucleotide between the two NBDs. This observation has done much to explain the obligatory cooperativity between the two NBDs during ATP hydrolysis and substrate transport by proteins such as P-glycoprotein (P-gp) and MRP1 (Senior and Bhagat, 1998; Hou et al., 2000; Hou et al., 2002; Gao et al., 2000; Payen et al., 2003; Urbatsch et al., 1998).

The catalytic cycle of ABC transporters is believed to involve alternating conformational changes between high-affinity substrate binding and low-affinity substrate releasing states. In the original model proposed for P-gp, the alternating ATP binding/hydrolysis and subsequent release of ADP by either NBD drives a single cycle through high- to low- to high-affinity states with the resultant transport of one molecule of substrate (Senior et al., 1995). More recently, it has been proposed that one ATP hydrolysis event results in conversion from the high- to low-affinity binding state and substrate transport, while hydrolysis of a second ATP is required to reset the protein in a high-affinity substrate binding conformation (Sauna and Ambudkar, 2001). Whether each NBD has a distinct role in the transport process has not been firmly established. Studies of P-gp, in which positions of NBDs were exchanged, suggest that the location of the NBD in the protein may influence its ability to bind and hydrolyze nucleotide (Beaudet and Gros, 1995; Hrycyna et al., 1999).

We and others have shown that in MRP1, the NBDs behave very differently with the respect to both ATP binding and hydrolysis. High-affinity binding of azido-ATP to NBD1 is

MOL #7708

readily demonstrable while under hydrolytic conditions in the presence of vanadate, ADP is trapped predominantly by NBD2 (Gao et al., 2000; Hou et al., 2000). Furthermore, binding of azido-ATP and the trapping of ADP by NBD2 requires that NBD1 be able to bind and possibly to hydrolyze ATP. In contrast, binding of ATP by NBD1 remains readily detectable when NBD2 is inactivated by mutations that eliminate ATP binding or ATPase activity (Gao et al., 2000; Hou et al., 2000). Studies with soluble forms of the NBDs support the ability of NBD1 to bind ATP with relatively high-affinity in the absence of NBD2 (Gao et al., 2000). Mutation of the Walker A motifs in each NBDs also has different effects on transport activity (Gao et al., 2000; Hou et al., 2000). Mutation of the conserved Walker A Lys residue in NBD1 only partially inactivates the protein while the comparable mutation in NBD2 essentially eliminates transport activity (Gao et al., 2000; Hou et al., 2000).

Recently, we demonstrated that the identity of the acidic residue COOH-proximal to the conserved Asp of the Walker B motif makes a critical contribution to the functional differences between the two NBDs (Payen et al., 2003). In NBD1 of MRP1 this residue is Asp and in NBD2 it is Glu, which is the residue found in the majority of ABC NBDs. Inter-conversion of these two residues profoundly affects the ability of the mutated NBDs to bind, hydrolyze and release nucleotides (Payen et al., 2003). A D793E mutation in NBD1 enhanced its hydrolytic capacity but caused occlusion of the resultant ADP by the mutant NBD1 in the absence of vanadate. The mutation also markedly decreased LTC<sub>4</sub> transport activity and resulted in an inability to shift from a high- to low-affinity LTC<sub>4</sub> binding state in the presence of ATP (Payen et al., 2003). The reciprocal E1455D mutation of NBD2 increased the affinity of NBD2 for both azido-ATP and -ADP, resulting in prolonged binding of both nucleotides. In the presence of ATP this mutation effectively locked the protein in a low-affinity substrate binding state. Based on these and other studies, we have proposed that transition from a high-affinity substrate binding state to a low-

MOL #7708

affinity substrate releasing state involves a conformational change that occurs following occupancy of NBD2 by ATP and persists as long as NBD2 is occupied by ADP. Furthermore, this transition apparently cannot occur when NBD1 is occupied by ADP rather than ATP (Payen et al., 2003).

In this study, we have investigated whether ATP hydrolysis by either NBD is essential for the conversion of MRP1 from a high- to low-affinity substrate binding state. To do so, we have examined the effects of various ATP analogs and the trapping of ADP in the presence of beryllium fluoride, on LTC<sub>4</sub> binding. We have also introduced mutations that have different effects on nucleotide binding and hydrolysis into each NBD and examined their influence on binding and transport of LTC<sub>4</sub>. The results support a model in which the transition from high- to low-affinity substrate binding requires occupancy of both NBDs by ATP. However, we also found that the non-hydrolysable ATP analogs, AMP-PNP and AMP-PCP, in contrast to ATP- $\gamma$ -S, are unable to substitute for ATP in driving the transition from high- to low-affinity binding. In addition, we show that mutations of the signature 'C' sequence which have no apparent effect on ATP binding, nevertheless, result in loss of the ability to shift from high to low-affinity states in the presence of ATP plus vanadate, or ATP- $\gamma$ -S. This observation suggests that the 'C' signature mutations affect transduction of conformational changes that occur in the NBDs following ATP binding, and which are required for the transition from high to low-affinity substrate binding states to occur.

## Materials and Methods

**Materials.** 8-azido [ $\alpha$ -<sup>32</sup>P] ATP, 8-azido [ $\gamma$ -<sup>32</sup>P] N<sub>3</sub> ATP were purchased from Affinity Labeling Technologies, Inc. (Lexington, KY, USA) ; specific activity between 5 and 20 Ci mmol<sup>-1</sup>).

MOL #7708

Beryllium, orthovanadate, ATP, AMP-PNP, AMP-PCP, ADP and ATP- $\gamma$ -S compounds were from Sigma Aldrich. [ $^3\text{H}$ ]LTC<sub>4</sub> was purchased from NEN (specific activity: 182 Ci mmol<sup>-1</sup>).

**MRP1 mutations.** The pFBdual-MRP1 1-932/932-1531 construct (pFBDual-halves, pFBDual-D123/D45) was cloned into pFASTBAC Dual (Life technologies Inc.). This construct, encoding the NH<sub>2</sub>-MSD1-MSD2-NBD1 and COOH-MSD3-NBD2 proximal half-molecules of MRP1, has been described (Gao et al., 1996; Gao et al., 2000). The amino acid substitutions within NBDs of MRP1 were generated by site-directed mutagenesis using the Clontech Transformer Kit (Clontech Laboratories, BD Biosciences, ON, Canada). The templates used for site-directed mutagenesis, pGEM-NBD1 and pGEM-NBD2, were described previously (Gao et al., 2000). The forward primers for creating K684R, K684E, K1333R, K1333E mutations of Walker A motifs were 5'-GGCTGCGGAAGGTCGTCCCTGC-3', 5'-GGGCTGCGGAGAGTCGTCCCTGC-3', 5'-GGGAGCTGGGAGGTCGTCCCTGA-3' and 5'-GGGAGCTGGGGAGTCGTCCCTGA-3', respectively. The forward primers for the G771A and G1433A mutations of signature sequences were 5'-CCTGTCTGGGGCCCAGAAGCAGC-3' and 5'-CCTCAGTGTGCGCGCAGCGCCAG-3', respectively. The forward primers for the D792N and D1454N mutations of the Walker B motifs were 5'-CATTTACCTCTTCAATGATCCCCTC-3' and 5'-ATCCTTGTGTTGAATGAGGCCACG-3', respectively. The presence of the mutation and the fidelity of the sequence of the MRP1 coding region were confirmed by dideoxy sequencing (ACGT Corporation, ON, Canada). The *Bsu36I*-*SphI* fragments bearing mutations at NBD1 were isolated from pGEM-NBD1 and used to replace the same region in pFBDual-halves to create pFBDual-halves/MutNBD1. The *EcoRI*-*KpnI* fragments with mutations at NBD2 were isolated from pGEM-NBD2 and used to replace the equivalent region in pBS-D45 to generate pBS-D45/MutNBD2. Then pBS-D45/MutNBD2 was digested with *NcoI* and *KpnI* and the *NcoI*-*KpnI* fragment was used to replace the equivalent region of pFBDual-D45 to give pFBDual-



MOL #7708

D45/MutNBD2. Finally, the *SalI-XbaI* fragment of pFBDual-halves was isolated and cloned into pFBDual-D45/MutNBD2, which had been digested with the same enzymes, to generate pFBDual-halves/MutNBD2.

**Viral infection, membrane vesicle preparation.** Viral infection of Sf21 cells was carried out as described (Gao et al., 1996; Gao et al., 2000). To generate membrane vesicles, Sf21 cells were disrupted by nitrogen cavitation and vesicles were subsequently isolated by discontinuous sucrose gradient density centrifugation (Leier et al., 1994; Loe et al., 1996).

**Immunoblotting and quantification of MRP1 polypeptides.** Membrane vesicle proteins were analyzed by SDS-polyacrylamide gel electrophoresis (PAGE) using 7-15% gradient gels. Proteins were transferred to Immobilon-P membranes (Millipore, Bedford, MA, USA) using 25 mM Tris-base, 192 mM glycine and 20% methanol buffer. MRP1 polypeptides were detected using an enhanced chemiluminescence Kit (ECL) (Amersham, Qu, Ca) and the murine mAb MRPm6 and the rat mAb MRPr1 (Pierce, Rockford, USA) (Flens et al., 1994; Hipfner et al., 1998). The relative levels of various mutant MRP1 polypeptides were estimated by comparison with vesicles containing wt MRP1. Densitometry of film images was performed using a ChemiImager<sup>TM</sup> 4000 (Alpha Innotech Corp., San Leandro, CA). The relative protein expression levels were calculated by dividing the integrated densitometry values obtained for 0.5, 1 and 2  $\mu$ g of total membrane protein from infected cells expressing the mutant proteins by the integrated densitometry values obtained for the comparable amounts of total membrane proteins from infected cells expressing the wt protein.

**Transport of [<sup>3</sup>H] LTC<sub>4</sub> into insect membrane vesicles.** Uptake of [<sup>3</sup>H] LTC<sub>4</sub> (50 nM, 182 Ci mmol<sup>-1</sup>, NEN) into membrane vesicles was measured at 23°C in the presence of ATP (4 mM), or AMP (4 mM) using a rapid filtration technique as previously described (Loe et al., 1996). Adjustment of wild type MRP1 levels in membrane vesicles subjected to photolabeling with

MOL #7708

**Photoaffinity labeling of MRP1 with [ $^3\text{H}$ ] LTC $_4$ .** Unless otherwise indicated in the figure legend, insect membrane vesicles (50  $\mu\text{g}$  total protein in 20  $\mu\text{l}$ ) were incubated with [ $^3\text{H}$ ] LTC $_4$  (0.13  $\mu\text{Ci}$ , 200 nM) at room temperature for 20 min. The vesicle samples were then frozen in liquid nitrogen (1 min) and subjected to UV-cross linking at 312 nm (1 min) in a Stratalinker Uv cross-linker. This process was repeated 10 times with each sample (Qian et al., 2001). Radiolabeled vesicles were then analyzed on SDS-PAGE (7-15%). Proteins were fixed by 25% isopropanol, 65% water and 10% acetic acid, for 30 min. Gels were then soaked in Amplify for 30 min and dried at 80°C for 2 hours, prior to auto-radiography using Kodak BioMax MS films (Qian et al., 2001).

**Photolabeling of NBD1 and NBD2 of MRP1 with 8-azido [ $^{32}\text{P}$ ] ATP.** 8-azido [ $\gamma$ - $^{32}\text{P}$ ] ATP or 8-azido [ $\alpha$ - $^{32}\text{P}$ ] ATP photoaffinity labeling was performed as described (Gao et al., 2000). Membrane vesicles (20  $\mu\text{g}$  total protein) were resuspended in transport buffer (50 mM Tris-HCl, pH7.4, 250 mM sucrose, and 0.02% of Na $_3\text{N}$ ) containing 5 mM MgCl $_2$ , and 5  $\mu\text{M}$  of 8-azido [ $^{32}\text{P}$ ] ATP. After 5 min at 4°C in a 96-well plate, the membranes were irradiated for 7 min on ice in a Stratalinker UV cross-linker ( $\lambda$ = 312 nm). After addition of 300  $\mu\text{l}$  of ice-cold buffer (50 mM Tris-HCl, pH 7.4, 0.1 mM EGTA and 5 mM MgCl $_2$ ), the membranes were centrifuged at 14,000 rpm for 15 min at 4°C. A second wash was performed and the pellets were resuspended in 14  $\mu\text{l}$  of ice-cold buffer. After addition of Laemmli buffer (4X), containing DTT (100 mM final), vesicle proteins were separated by SDS-PAGE using 7-15% gradient gels. After drying for 2 hours at 80°C, gels were subjected to autoradiography either using a PhosphorImager (Molecular Dynamics, Inc) and/or by exposure to Kodak BioMax MS films.

**Vanadate and beryllium fluoride induced trapping of 8-azido [ $\alpha$ - $^{32}\text{P}$ ] ADP by MRP1.**

Membrane vesicles (20  $\mu\text{g}$  protein) were resuspended in transport buffer containing 5 mM of

MOL #7708

MgCl<sub>2</sub>, and 15  $\mu$ M 8-azido [ $\alpha$ -<sup>32</sup>P] ATP. The 15 min incubation at 37°C was performed in the presence or absence of 1 mM vanadate or 200  $\mu$ M beryllium fluoride. The reaction was started by addition of 8-azido [ $\alpha$ -<sup>32</sup>P] ATP and stopped by transfer on ice and addition of ice-cold buffer as previously described. Unreacted nucleotides were then removed (2X) by addition of 300  $\mu$ L of ice-cold buffer followed by centrifugation. Pellets were resuspended in 14  $\mu$ L of ice-cold buffer and vesicle membranes were irradiated for 7 min on ice in a Stratalinker UV cross-linker ( $\lambda$ = 312 nm) as previously described (Gao et al., 2000). After the addition of Laemmli buffer (4X), containing DTT (100 mM final), membrane vesicles were separated by gradient SDS-PAGE (7-15%). After drying for 2h at 80°C, gels were processed as described above.

## Results

**Effect of nucleotide analogs on photolabeling of MRP1 by [<sup>3</sup>H] LTC<sub>4</sub>.** We have shown that LTC<sub>4</sub> photolabels MRP1 predominantly in MSD2 and to a lesser extent in MSD3 (Qian et al., 2001; Gao et al., 1998). The extent of photolabeling, particularly of the site in MSD2, is also moderately attenuated in the presence of ATP and strongly attenuated in the presence of ATP plus vanadate (Payen et al., 2003; Qian et al., 2001). Based on these and more recent studies with mutant proteins, we have proposed that it is the occupancy of NBD2 by either ATP or ADP that maintains MRP1 in a low-affinity state. To further investigate this proposal, we have examined the effect of non-hydrolyzable ATP analogs, AMP-PNP and AMP-PCP, as well as beryllium-induced ADP trapping, on the binding of LTC<sub>4</sub>.

At 23°C, in the presence of ATP or ATP plus vanadate, LTC<sub>4</sub> photolabeling by wt MRP1 was decreased by approximately 55% and 75%, respectively (Fig. 1A). As observed previously, ATP- $\gamma$ -S, a poorly hydrolyzable analog of ATP, also caused a moderate (43%) decrease in LTC<sub>4</sub> binding, similar to that of ATP in the absence of vanadate (Fig. 1A). We also examined the effect

MOL #7708

of beryllium fluoride on LTC<sub>4</sub> photolabeling, since ADP trapping in the presence of beryllium fluoride results in a NBD conformation closely resembling that of an ATP binding ground state, rather than the post-hydrolytic transition state formed in the presence of orthovanadate (Sankaran et al., 1997; Fisher et al., 1995; Smith and Rayment, 1996). The combination of ATP and beryllium fluoride reduced LTC<sub>4</sub> labeling by approximately 80% and thus was at least as effective as ATP plus vanadate (Fig. 1A). These results combined with those obtained with ATP- $\gamma$ -S strongly support the suggestion that the decrease in LTC<sub>4</sub> binding occurs upon ATP binding. However, since ATP- $\gamma$ -S can be slowly hydrolyzed, we examined the ability of two completely non-hydrolyzable analogs, AMP-PNP and AMP-PCP, to shift MRP1 from a high- to low-affinity state. Neither analog decreased labelling by LTC<sub>4</sub> (Fig. 1A). In view of this result, we compared the ability of ATP- $\gamma$ -S and AMP-PNP to compete with azido-ATP for binding to the NBDs of MRP1 (Fig. 1B). ATP- $\gamma$ -S competed for photolabeling of both NBDs by 8-azido [  $\gamma$  -<sup>32</sup>P] ATP (5  $\mu$ M), with competition being detectable at the lowest concentration used (5  $\mu$ M). In contrast, AMP-PNP was at least 20 fold less effective, particularly at competing for binding to NBD2, where no competition was evident at concentrations up to 100  $\mu$ M (Fig. 1B). However, at a concentration of 1mM, as used in the LTC<sub>4</sub> labeling studies, AMP-PNP decreased 8-azido [  $\gamma$  -<sup>32</sup>P] ATP photolabeling of both NBDs by more than 90%. Thus the lack of an effect on labelling of MRP1 by LTC<sub>4</sub> cannot simply be attributed to a failure of the analog to bind to the protein at the concentration used.

**Effect of conservative and non-conservative mutations of the Walker A lysine residue in NBD1 and NBD2 on LTC<sub>4</sub> transport.** Mutation of the conserved Walker A Lys684 in NBD1 to Met substantially reduces but does not eliminate MRP1 transport activity while the comparable mutation in NBD2, K1333M, essentially inactivates the protein (Gao et al., 2000; Hou et al., 2000). Despite retention of ~30% of wt LTC<sub>4</sub> transport activity by the K684M mutant protein, we

MOL #7708

were unable to detect photolabeling of either NBD with 8-azido-ATP (Gao et al., 2000).

Comparable mutations in other ABC transporters uniformly eliminate ATPase activity at the mutated NBD but have variable effects on ATP binding depending on the nature of the substitution (Shyamala et al., 1991, Schneider et al., 1994, Urbatsch et al., 1998). Consequently, we compared the effect of introducing conservative Lys to Arg and opposite charge Lys to Glu mutations at positions 684 and 1333 on both transport activity and ATP binding. Mutant half-molecules containing these substitutions were expressed with the appropriate wt half-molecule using dual-expression vectors.

Densitometry of immunoblots of vesicle proteins indicated that levels of the K684R, K684E, K1333R and K1333E MRP1 mutants ranged from 30-60% those of wt MRP1 (Fig. 3A). Consequently, ATP-dependent transport of LTC<sub>4</sub> was normalized to the expression level of wt MRP1. Notably, the K684R substitution in NBD1 decreased ATP-dependent LTC<sub>4</sub> uptake by only 40% while the K1333R mutation in NBD2 reduced transport by approximately 80% (Fig. 3B). In contrast, the non-conservative Walker A Lys to Glu mutation in either NBD decreased ATP dependent LTC<sub>4</sub> uptake by >90% (Fig. 3B).

**Effect of mutations of Walker A Lys on ATP binding and vanadate induced ADP trapping.** The membrane vesicles used in the transport assays described above were also used for binding and photolabeling studies with 8-azido [ $\gamma$ -<sup>32</sup>P] ATP (Fig. 3C). For binding experiments, the levels of wt MRP1 which were 2-3 fold higher than in membranes containing the mutant proteins, were adjusted by dilution with  $\beta$ -gus control vesicles so that close to comparable amounts of total protein and MRP1 half-molecules (wt or mutant) were subjected to photolabeling (Fig. 3C and D). The K684E mutation markedly decreased binding at both the mutant NBD1 and the wt NBD2, as observed previously with the Met mutation (Gao et al., 2000). The conservative K684R mutation also decreased photolabeling of both NBDs, but to a

MOL #7708

lesser extent than either the Asp or Met mutations (Fig. 3C). In contrast, both the K1333R and the K1333E mutations essentially eliminated binding at NBD2 while having little or no effect on the labeling of NBD1 (Fig. 3C).

Under vanadate trapping conditions the majority of ADP is trapped at NBD2 of the wt protein (Fig. 3D). Both the conservative and non-conservative K684 mutations markedly reduced trapping at the associated wt NBD2 and no difference between them was apparent. Similarly, both the K1333R and K1333E mutations eliminated trapping by the mutant NBD2 (Fig. 3D). Thus despite the difference in extent to which the conservative and non-conservative mutations compromise LTC<sub>4</sub> transport, all mutations essentially eliminate the ability to detect vanadate dependent ADP trapping by NBD2.

**Effect of mutations of Walker A Lys on LTC<sub>4</sub> photolabeling.** As an alternative approach to assessing the effect of the Walker A mutations on the function of MRP1, we examined LTC<sub>4</sub> binding in the presence and absence of ATP, ATP/vanadate and ATP- $\gamma$ -S (Fig. 4). This approach enabled much higher nucleotide concentrations to be used than is feasible for nucleotide photolabeling studies with <sup>32</sup>P-labeled derivatives. In the absence of nucleotides, the mutant proteins displayed an LTC<sub>4</sub> labeling profile very similar to that of wt protein. However, in the presence of ATP, ATP/vanadate and ATP- $\gamma$ -S, none of the Walker A Lys mutants displayed the reduction in LTC<sub>4</sub> labeling observed with wt MRP1 (Fig. 4).

**Effect of mutations of Walker B Asp on LTC<sub>4</sub> transport, ATP photolabeling, vanadate induced ADP trapping and LTC<sub>4</sub> binding.** Substitution of the conserved Asp residue in the Walker B motif has been shown in several ABC proteins to result in loss of both ATP binding and hydrolysis (Shyamala et al., 1991; Ueda et al., 1997; Hrycyna et al., 1999). This residue in both NBDs was converted to polar Asn and the mutant half-molecules were co-expressed with the appropriate wt partner (Fig. 2). The D792N mutation diminished transport activity by

MOL #7708

approximately 65% while the D1454N mutation essentially inactivated the protein (Fig. 5B). As observed with the NBD1 Walker A mutations, the D792N mutation drastically decreased binding by NBD1 and to a lesser extent binding by NBD2. In contrast, the D1454N mutation eliminated photolabeling of only NBD2 and had no effect on photolabeling of NBD1 (Fig. 5C). The D792N mutation also strongly decreased ADP trapping by both NBD1 and NBD2, while the D1454N mutation eliminated trapping by NBD2 but only modestly decreased trapping by NBD1 (Fig. 6B). Despite the partial retention of vanadate dependent trapping at NBD2 of the D792N mutant, we were unable to detect an ATP/vanadate dependent decrease in LTC<sub>4</sub> binding with either mutant (Fig. 6C).

#### **Effect of mutation of the invariant Gly in the ABC signature sequences of NBD1 and NBD2.**

The invariant Gly at the fourth position of the ABC signature sequence in each of the NBDs was mutated to Ala to minimize changes in the bulk and chemical characteristics of the amino acid (Fig. 2). The G771A and G1433A mutants were expressed at 90% and 50%, respectively, of the level of wt MRP1. The levels of ATP-dependent LTC<sub>4</sub> transport activity and the MRP1 content of proteins samples used for nucleotide photolabeling studies were normalized to that of wt MRP1 as described above (Fig. 7A).

In contrast to the results obtained with the Walker A and B mutants, the NBD1 ABC signature mutation, G771A, eliminated LTC<sub>4</sub> transport while the NBD2 G1433A mutant retained approximately 30% of the activity of the wt protein (Fig. 7B). Also unlike the Walker A and B mutations, neither of the NBD1 or NBD2 signature mutations decreased the binding and photolabeling of the protein by 8-azido [ $\gamma$ -<sup>32</sup>P] ATP (Fig. 7C). Under vanadate induced trapping conditions, both the G771A and G1433A mutations markedly decreased trapping of ADP at NBD2, but had relatively little effect on the low level of trapping typically observed at NBD1 (Fig. 7D). However, like the Walker A and B mutations, the signature sequence mutations

MOL #7708

eliminated the decrease in LTC<sub>4</sub> photolabeling observed in the presence of ATP- $\gamma$ -S and ATP/vanadate (Fig. 8).

## Discussion

Crystal structures of ABC NBDs indicate that the generally conserved Glu residue following the Walker B motif interacts with bound Mg<sup>++</sup> and a water molecule that are essential for cleavage of the  $\beta$ - $\gamma$ -phosphodiester bond of ATP (Moody et al., 2002; Smith et al., 2002; Verdon et al., 2003). Although the COOH-proximal NBDs of ABCC proteins contain the conserved Glu, the NH<sub>2</sub>-proximal NBDs do not. In MRP1 NBD1, the corresponding residue is Asp and in other ABCC proteins, is an uncharged residue. We have recently shown that the lack of a Glu residue at this location in NBD1 is a major contributor to differences in functional characteristics of the two NBDs of ABCC proteins (Payen et al., 2003). A Glu to Asp mutation in NBD2 drastically decreases ATP hydrolysis and release of both ATP and ADP (Payen et al., 2003). Since this mutation strongly potentiates the decrease in LTC<sub>4</sub> photolabeling observed in the presence of either ATP or ATP- $\gamma$ -S, we have proposed that MRP1 exists in a low affinity substrate binding state when NBD2 is occupied by either ATP or ADP (Payen et al., 2003). That fact that beryllium fluoride and orthovanadate are equally effective in potentiating the shift to a low-affinity LTC<sub>4</sub> binding state, strongly supports our suggestion that the decrease in substrate affinity occurs upon binding of ATP to NBD2 and persists in the transition state following cleavage of the  $\gamma$ -phosphate (Fig. 1A).

To confirm that ATP hydrolysis by NBD2 was not required to shift the protein to a low-affinity state we used two non-hydrolyzable analogs, AMP-PNP and AMP-PCP. However, neither AMP-PNP nor AMP-PCP caused a detectable decrease in photolabeling of MRP1 with



MOL #7708

LTC<sub>4</sub>. Although this might suggest that ATP hydrolysis is required for the decrease in LTC<sub>4</sub> binding to occur, the extent to which these analogs fully mimic ATP appears to be transporter dependent. AMP-PNP has been reported to decrease affinity of Chinese hamster P-gp for vinblastine (Martin et al., 2001), but this analog failed to decrease binding of [<sup>125</sup>I] iodoarylazidoprazosine by the human protein (Sauna and Ambudkar, 2000). Similarly, AMP-PNP does not promote homodimerization of the bacterial ABC NBDs, MJ0796 and MJ1267 (Moody et al., 2002), nor does it elicit an ATP-dependent, SecA coupled conformational change in SecYEG, the bacterial complex involved in preprotein extrusion. In this case, only one AMP-PNP binding site could be detected, suggesting that the NBD dimer formed an abnormal interface that did not generate a second binding site for the ortholog (Tziatzios et al., 2004).

AMP-PNP and AMP-PCP contain a nitrogen and carbon atom, respectively, between the  $\beta$  and  $\gamma$  phosphate moieties. In contrast, the  $\beta$ - $\gamma$  phosphodiester bond of ATP is unchanged in ATP- $\gamma$ -S. This may be critical for formation of the correct dimer interface between NBDs of some ABC proteins. Clearly, ATP- $\gamma$ -S competes much more effectively than AMP-PNP for binding of azido-ATP by MRP1. ATP- $\gamma$ -S also stimulates ADP trapping at NBD2 of MRP1 and thus mimics ATP binding by NBD1, but analogs such as AMP-PNP do not (Hou et al., 2002). Consequently, the failure of AMP-PNP to decrease the affinity of MRP1 for LTC<sub>4</sub> could be attributable to the fact that it fails to accurately simulate ATP when interacting with one or both binding sites on the NBD dimer.

To further characterize the influence of nucleotide interactions on changes in substrate binding by MRP1, we created mutations in conserved elements in each NBD that had different effects on transport activity, ATP binding and ADP trapping. Any substitution of the invariant Walker A Lys in ABC NBDs generally abolishes ATP hydrolysis (Hou et al., 2000; Urbatsch et al., 1998; Gao et al., 2000), but the effect on nucleotide binding depends on whether the mutation

MOL #7708

is conservative or non-conservative (Shyamala et al., 1991; Schneider et al., 1994). In several ABC NBDs, substitutions of the conserved Walker B Asp residue that eliminate the negatively charged side chain have been shown to abolish both ATP hydrolysis and to strongly decrease nucleotide binding (Shyamala et al., 1991., Ueda et al., 1997; Hrycyna et al., 1999). Consistent with the retention of partial activity by NBD1 Walker A Lys mutations being attributable to a greater or lesser ability to bind ATP, LTC<sub>4</sub> transport was decreased only 40% by a conservative Arg mutation while the opposite charge Glu mutation decreased activity by more than 90%. By comparison, the previously described Lys to Met mutation in NBD1 resulted in a 70% decrease in LTC<sub>4</sub> transport. These results support the suggestion that some level of transport activity can be retained providing NBD1 is capable of binding, but not necessarily, hydrolyzing ATP. In contrast, both conservative and non-conservative mutations in NBD2 decreased transport by at least 80%. Despite differences in the level of transport activity, conservative and non-conservative NBD1 Walker A mutations drastically reduced ATP binding and vanadate dependent trapping of ADP by NBD2. In contrast, the comparable NBD2 mutations had little effect on ATP binding by the co-expressed wt NBD1 although they eliminated azido-ATP binding and ADP trapping by the mutant NBD2. The effect of the MRP1 Walker B D792N and D1454N mutations on ATP binding and ADP trapping was similar to that of the Walker A Lys mutations, with the level of transport activity of the NBD1 Asp to Asn mutation being comparable to that of the Walker A Lys to Met mutation (Gao et al., 2000).

The Walker A and B mutations confirm the strong dependence of ATP binding at NBD2 on the binding of ATP to NBD1. They also indicate that initial ATP binding by NBD1 is relatively independent of the ability of NBD2 to bind nucleotide. However, despite retention of partial transport activity by the NBD1 mutant proteins, particularly following the conservative Walker A Lys to Arg mutation, no decrease in LTC<sub>4</sub> binding in the presence of ATP plus

MOL #7708

vanadate was detectable. This observation was unexpected since the LTC<sub>4</sub> binding experiments are carried out at ATP concentrations comparable to those used for transport. Why we were unable to detect a decrease in LTC<sub>4</sub> binding is presently not known. It is possible that the NBD1 Walker A and B mutations result in very transient formation of the low-affinity binding state that we are unable to detect with a photolabeling ligand such as LTC<sub>4</sub>, which requires relatively long exposure times. Studies with other more efficient photoligands may resolve this issue.

In contrast to Walker A and B mutations, substitution of conserved residues in the signature sequences of a number of ABC proteins has been found to have little effect on ATP binding (Schmees et al., 1999; Shyamala et al., 1991; Tomblin et al., 2004). Recent studies of MRP1 in which conserved signature Gly residues were mutated to Glu, indicated that ATP binding by the mutant proteins was apparently normal. However, the proteins were inactive and failed to trap ADP in the presence of vanadate suggesting that the Gly residues are essential for the formation of a post-hydrolytic complex (Szentpetery et al., 2004). Consequently, we investigated whether such mutant proteins differed from the Walker A and B mutants in their ability to shift from a high to low-affinity binding state in the presence of ATP or ATP- $\gamma$ -S.

Despite the more conservative Gly-Ala, as opposed to Gly-Glu, substitutions used in the present study, the NBD1 mutation essentially inactivated the protein while the mutation in NBD2 decreased LTC<sub>4</sub> transport activity by approximately 70%. Thus the relative effect of signature sequence mutations NBD1 and NBD2 on transport is the converse of the Walker A and B mutations, as might be expected if the signature sequence contributes to ATP hydrolysis by the apposed NBD. As observed with the signature Gly to Glu mutations in MRP1 (Szentpetery et al., 2004), the Gly-Ala mutations had little or no effect on binding of ATP by either the NBD containing the mutation or the apposing wt NBD. However, both NBD mutations strongly decreased but did not eliminate vanadate dependent trapping at NBD2, while the low level of

MOL #7708

trapping observed at NBD1 in the wt protein was relatively unaffected. Although nucleotide binding at NBD1 and NBD2, as well as vanadate dependent trapping at NBD1, were apparently unaffected, both signature Gly mutations eliminated the shift to a low-affinity substrate binding state, not only in the presence of ATP and vanadate, but also in the presence of ATP- $\gamma$ -S. These observations suggest that formation of a closed dimer as a result of ATP binding to both NBD1 and NBD2 may not be sufficient to mediate the conformational shift from high to low-affinity. They also raise the possibility that other pre-hydrolytic conformational changes involving interaction of the signature Gly residue with the  $\gamma$ -phosphate of ATP are required for the shift in affinity for substrate to occur. If so, the failure of ATP analogs such as AMP-PNP to induce changes in substrate binding, may also be related to an inability to establish the necessary interactions with highly conserved residues in the signature sequence.

*Acknowledgements* - We thank our colleagues Drs. Caroline Grant and Gwenaëlle Conseil for helpful discussions and advice. The excellent technical assistance from Monika Vasa and Ruth Burtch-Wright is also acknowledged.

MOL #7708

## References

- Beaudet L and Gros P (1995) Functional dissection of p-glycoprotein nucleotide-binding domains in chimeric and mutant proteins. Modulation of drug resistance profiles. *J Biol Chem* **270**:17159-17170.
- Chang G (2003) Structure of MsbA from *Vibrio cholera*: a multidrug resistance ABC transporter in a closed conformation. *J Mol Biol*, **330**: 419-430.
- Cole SP, Bhardwaj G, Gerlach JH, Mackie JE, Grant CE, Almquist KC, Stewart AJ, Kurz EU, Duncan AM and Deeley RG (1992) Overexpression of a transporter gene in a multidrug resistant human lung cancer cell line. *Science* **258**:1650-1654.
- Cole SP, Sparks KE, Fraser K, Loe DW, Grant CE, Wilson GM and Deeley RG (1994) Pharmacological characterization of multidrug resistant MRP-transfected human tumor cells. *Cancer Res* **54**:5902-5910.
- Dean M and Allikmets R. (2001) Complete characterization of the human ABC gene family. *J Bioenerg Biomembr* **33**:475-479.
- Diederichs K, Diez J, Grellner G, Muller C, Breed J, Schnell C, Vonnheim C, Boos W and Welte W (2000) Crystal structure of MalK, the ATPase subunit of the trehalose/maltose ABC transporter of the archaeon *thermococcus litoralis*. *EMBO J* **19**:5951-5961.
- Fisher AJ, Smith CA, Thoden JB, Smith R, Sutoh K, Holden HM and Rayment I (1995) X-ray structures of the myosin motor domain of dictyostelium discoideum complexed with MgADP.BeFx and MgADP.AIF<sub>4</sub><sup>-</sup>. *Biochemistry* **34**:8960-8972.

MOL #7708

Flens MJ, Izquierdo MA, Scheffer GL, Fritz JM, Meijer CJ, Scheper RJ and Zaman GJ (1994)

Immunochemical detection of the multidrug resistance-associated protein MRP in human multidrug-resistant tumor cells by monoclonal antibodies. *Cancer Res* **54**:4557-4563.

Gao M, Loe DW, Grant CE, Cole SP and Deeley RG (1996) Reconstitution of ATP-dependent leukotriene C<sub>4</sub> transport by co-expression of both half-molecules of human multidrug resistance protein in insect cells. *J Biol Chem* **271**:27782-27787.

Gao M, Yamazaki M, Loe DW, Westlake CJ, Grant CE, Cole SP and Deeley RG (1998) Multidrug resistance protein. Identification of regions required for active transport of leukotriene C<sub>4</sub>. *J Biol Chem* **273**:10733-10740.

Gao M, Cui HR, Loe DW, Grant CE, Almquist KC, Cole SP and Deeley RG (2000) Comparison of the functional characteristics of the nucleotide binding domains of multidrug resistance protein 1. *J Biol Chem* **275**:13098-13108.

Gaudet R and Wiley DC (2001) Structure of the ABC ATPase domain of human TAP1, the transporter associated with antigen processing. *EMBO J* **20**: 4964-4972.

Hipfner DR, Almquist KC, Leslie EM, Gerlach JH, Grant CE, Deeley RG and Cole SPC (1997) Membrane topology of the multidrug resistance protein (MRP). A study of glycosylation-site mutants reveals an extracytosolic NH<sub>2</sub> terminus. *J Biol Chem* **272**:23623-23630.

Hipfner DR, Gao M, Scheffer G, Scheper RJ, Deeley RG and Cole SP (1998) Epitope mapping of monoclonal antibodies specific for the 190-kDa multidrug resistance protein (MRP). *Br J Cancer* **78**:1134-1140.

MOL #7708

Hopfner KP and Tainer JA (2003) Rad50/SMC proteins and ABC transporters: unifying concepts from high-resolution structures. *Curr Opin Struct Biol* **13**:249-255.

Hou Y, Cui L, Riordan JR and Chang X (2000) Allosteric interactions between the two non-equivalent nucleotide binding domains of multidrug resistance protein MRP1. *J Biol Chem* **275**:20280-20287.

Hou YX, Cui L, Riordan JR and Chang XB (2002) ATP-binding to the first nucleotide-binding domain of multidrug resistance protein MRP1 increases binding and hydrolysis of ATP and trapping of ADP at the second domain. *J Biol Chem* **277**:5110-5119.

Hrycyna CA, Ramachandra M, Germann UA, Cheng PW, Pastan I and Gottesman MM (1999) Both ATP sites of human P-glycoprotein are essential but not symmetric. *Biochemistry* **38**:13887-13899.

Hung LW, Wang IX, Nikaido K, Liu PQ, Ames GF and Kim SH (1998) Crystal structure of the ATP-binding subunit of an ABC transporter. *Nature* **396**:703-707.

Kast C and Gros P (1997) Topology mapping of the amino-terminal half of multidrug resistance-associated protein by epitope insertion and immunofluorescence. *J Biol Chem* **272**: 26479-26487.

Leier I, Jedlitschky G, Buchholz U, Cole SP, Deeley RG and Keppler D (1994) The MRP gene encodes an ATP-dependent export pump for leukotriene C<sub>4</sub> and structurally related conjugates. *J Biol Chem* **269**:27807-27810.

Locher KP, Lee AT and Rees DC (2002) The E.coli BtuCD structure: a framework for ABC transporter architecture and mechanism. *Science* **296**:1091-1098.

MOL #7708

Martin C, Higgins CF and Callaghan R (2001) The vinblastine binding site adopts high- and low-affinity conformations during a transport cycle of P-glycoprotein. *Biochemistry* **40**:15733-15742.

Moody JE, Millen L, Binns D, Hunt JF and Thomas PJ (2002) Cooperative, ATP-dependent association of the nucleotide binding cassettes during the catalytic cycle of ATP-binding cassette transporters. *J Biol Chem* **277**:21111-21114.

Payen LF, Gao M, Westlake CJ, Cole SP and Deeley RG (2003) Role of carboxylate residues adjacent to the conserved core Walker B motifs in the catalytic cycle of multidrug resistance protein 1 (ABCC1). *J Biol Chem* **278**:38537-38547.

Qian YM, Qiu W, Gao M, Westlake CJ, Cole SP and Deeley RG (2001) Characterization of binding of leukotriene C<sub>4</sub> by human multidrug resistance protein 1: evidence of differential interactions with NH<sub>2</sub>- and COOH-proximal halves of the protein. *J Biol Chem* **276**:38636-38644.

Sankaran B, Bhagat S and Senior AE (1997) Inhibition of P-glycoprotein ATPase activity by beryllium fluoride. *Biochemistry* **36**:6847-6853.

Sauna ZE and Ambudkar SV (2000) Evidence for a requirement for ATP hydrolysis at two distinct steps during a single turnover of the catalytic cycle of human P-glycoprotein. *Proc Natl Acad Sci USA* **97**:2515-2520.

Sauna ZE and Ambudkar SV (2001) Characterization of the catalytic cycle of ATP hydrolysis by human P-glycoprotein. The two ATP hydrolysis events in a single catalytic cycle are kinetically similar but affect different functional outcomes. *J Biol Chem* **276**:11653-11661.



MOL #7708

Schmees G, Stein A, Hunke S, Landmesser H and Schneider E (1999) Functional consequences of mutations in the conserved 'signature sequence' of the ATP-binding-cassette protein MalK. *Eur J Biochem* **266**:420-430.

Schneider E, Wilken S and Schmid R (1994) Nucleotide-induced conformational changes of MalK, a bacterial ATP binding cassette transporter protein. *J Biol Chem* **269**:20456-20461.

Senior AE, al Shawi MK and Urbatsch IL (1995) The catalytic cycle of P-glycoprotein. *FEBS Lett* **377**:285-289.

Senior AE and Bhagat S (1998) P-glycoprotein shows strong catalytic cooperativity between the two nucleotide sites. *Biochemistry* **37**:831-836.

Shyamala V, Baichwal V, Beall E and Ames GF (1991) Structure-function analysis of the histidine permease and comparison with cystic fibrosis mutations. *J Biol Chem* **266**:18714-18719.

Smith CA and Rayment I (1996) X-ray structure of the magnesium(II).ADP.vanadate complex of the Dictyostelium discoideum myosin motor domain to 1.9 Å resolution. *Biochemistry* **35**:5404-5417.

Smith PC, Karpowich N, Millen L, Moody JE, Rosen J, Thomas PJ and Hunt JF (2002) ATP binding to the motor domain from an ABC transporter drives formation of a nucleotide sandwich dimer. *Mol Cell* **10**:139-149.

Szentpetery Z, Kern A, Liliom K, Sarkadi B, Varadi A and Bakos E (2004) The role of the conserved glycines of ABC signature motifs of MRP1 in the communications between the substrate binding site and the catalytic centers. *J Biol Chem*, in press.

MOL #7708

Tomblin G, Bartholomew L, Gimi K, Tyndall GA and Senior AE (2004) Synergy between conserved ABC signature Ser residues in P-glycoprotein catalysis. *J Biol Chem* **279**:5363-5373.

Tziatzios C, Schubert D, Lotz M, Gundogan D, Betz H, Schagger H, Haase W, Duong F and Collinson I (2004) The bacterial protein-translocation complex: SecYEG dimers associate with one or two SecA molecules. *J Mol Biol* **340**:513-524.

Ueda K, Inagaki N and Seino S (1997) MgADP antagonism to Mg<sup>2+</sup>-independent ATP binding of the sulfonylurea receptor SUR1. *J Biol Chem* **272**:22983-22986.

Urbatsch IL, Beaudet L, Carrier I and Gros P (1998) Mutations in either nucleotide-binding site of P-glycoprotein (Mdr3) prevent vanadate trapping of nucleotide at both sites. *Biochemistry* **37**:4592-4602.

Verdon G, Albers SV, van Oosterwijk N, Dijkstra BW, Driessen AJ and Thunnissen AM (2003) Formation of the productive ATP-Mg<sup>2+</sup>-bound dimer of GlcV, an ABC-ATPase from *Sulfolobus solfataricus*. *J Mol Biol* **334**:255-267.

## Footnotes

This work was supported by grants from the National Cancer Institute of Canada (NCIC) with funds from the Terry Fox Run and the Canadian Institutes of Health Research (CIHR, MT-10519) and a post-doctoral fellowship to L. Payen from CIHR.

MOL #7708

## Figure Legends

**Fig. 1.** Photolabeling of MRP1 with LTC<sub>4</sub> and 8-azido-[ $\gamma$ -<sup>32</sup>P] ATP. *A) Effect of ATP analogs, and ADP trapping on [<sup>3</sup>H]LTC<sub>4</sub> photolabeling of wt MRP1.* Membrane vesicles containing wt MRP1 (50  $\mu$ g total protein) were incubated in transport buffer alone at 23°C for 20 min, or transport buffer containing one of the following: ATP- $\gamma$ -S (4 mM), AMP-PNP (4 mM), AMP-PCP (4 mM), ATP (1 mM), or ATP (1 mM) plus either vanadate (1 mM) or BeF (200  $\mu$ M), prior to addition of [<sup>3</sup>H]LTC<sub>4</sub> (200 nM, 0.13  $\mu$ Ci). The [<sup>3</sup>H]LTC<sub>4</sub> photolabeling was performed as described under “Materials and Methods”. Similar results were obtained in at least three additional independent experiments. The relative levels of photolabeling by LTC<sub>4</sub> as determined by densitometry are indicated. *B) Effect of ATP analogs on photolabeling of MRP1 by 8-azido-[ $\gamma$ -<sup>32</sup>P] ATP.* Membrane vesicles (20  $\mu$ g total protein) were incubated with 8-azido-[ $\gamma$ -<sup>32</sup>P] ATP (5  $\mu$ M) for 5 min at 4°C in transport buffer in the absence (-) or presence of various concentrations (5  $\mu$ M to 1 mM) of ATP- $\gamma$ -S or AMP-PNP. The samples were photo-cross-linked and unincorporated nucleotides were removed as described under “Materials and Methods”. Similar results were obtained in at least two independent experiments. The positions of the labeled NH<sub>2</sub>- and COOH-halves of MRP1, containing NBD1 and NBD2, respectively, are indicated.

**Fig. 2.** Alignment of the amino acid sequences of NBD1 and NBD2 of MRP1. The sequence alignment was generated using ClustalW. Amino acids that are identical in both NBDs are bolded and conserved motifs are boxed. Amino acids mutated in the studies described are shown in white on a black background and indicated by ▲.

MOL #7708

**Fig. 3.** Effects of conservative and non-conservative mutations of Walker A Lys residues. *A) Expression levels of wt and mutant half-molecules.* Membrane vesicles (1  $\mu$ g total protein) prepared from Sf21 cells expressing a combination of a wt and mutant half molecule containing a K684E, K684R, K1333E, or K1333R mutation were separated by SDS-PAGE on gradient gels and transferred to Immobilon-P membranes. Membrane vesicles expressing both wt type halves of MRP1 were diluted with control membranes from cells expressing  $\beta$ -gus, as described in Materials and Methods and indicated in the figure, and 1  $\mu$ g of total protein was subjected to SDS-PAGE. *Left;* detection of the NH<sub>2</sub>-proximal half-molecule by rat MRP1-specific mAb MRPr1. *Right;* detection of COOH-proximal half-molecule by murine MRP1-specific mAb MRPM6. Minor amounts of high molecular weight species present in COOH-proximal half-molecule blot are oligomers of the half-molecules. The relative expression levels of wt and mutant proteins evaluated by densitometry are indicated in the figure. *B) Effect of K684E, K684R, K1333E and K1333R mutations on ATP-dependent LTC<sub>4</sub> transport activity.* Membrane vesicles (2  $\mu$ g total protein) containing either both wt, or a combination of wt and mutant, MRP1 half-molecules, together with control vesicles from cells expressing  $\beta$ -Gus vector were assayed for ATP-dependent LTC<sub>4</sub> transport activity as described. Results shown are means  $\pm$  S.D. of triplicate determinations in a single experiment. Similar results were obtained in at least three additional independent experiments. *C) Comparison of nucleotide binding by wt and mutant MRP1 half-molecules* Membrane vesicles (20  $\mu$ g total protein) containing either both wt, or a combination of wt and mutant, MRP1 half-molecules were incubated with 8-azido [ $\gamma$ -<sup>32</sup>P] ATP (5  $\mu$ M) for 5 min at 4°C in transport buffer prior to photo crosslinking and removal of unincorporated nucleotides, as described. Similar results were obtained in at least three independent experiments. The positions of NH<sub>2</sub>- and COOH-halves of MRP1 and labeled

MOL #7708

endogenous proteins (E►) are indicated. *D) Vanadate dependent ADP trapping by wt and mutant MRP1 half-molecules.* Samples of membrane vesicles used in *C)* were incubated in transport buffer containing 8-azido [ $\alpha$ - $^{32}$ P] ATP (15  $\mu$ M) for 15 min at 37°C in the absence (-) or presence (+) of 1 mM vanadate. Unbound nucleotides were removed prior to crosslinking and analysis by SDS-PAGE, as described. The positions of NH<sub>2</sub>- and COOH-halves of MRP1 and endogenous labeled proteins (E►) are indicated. Similar results were obtained in at least two independent experiments.

**Fig. 4.** Effect of conservative and non-conservative mutations of Walker A Lys residues on [ $^3$ H]LTC<sub>4</sub> photolabeling in the presence of either ATP plus vanadate or ATP- $\gamma$ -S. Membrane vesicles (50  $\mu$ g total protein) containing wt and the K684R, K684E, K1333R, K1333E mutant MRP1 half-molecules were incubated in transport buffer at 23°C for 20 min in the absence or presence of ATP- $\gamma$ -S (4 mM), or ATP (1 mM) plus vanadate (1 mM), prior to addition of [ $^3$ H]LTC<sub>4</sub> (200 nM, 0.13  $\mu$ Ci). [ $^3$ H]LTC<sub>4</sub> photolabeling was performed as described. Similar results were obtained in 4 additional independent experiments.

**Fig. 5.** Effect of Walker B Asp mutations on transport activity and nucleotide binding.

*A) Expression levels of wt and mutant half-molecules of MRP1.* Vesicle proteins were separated by SDS-PAGE and immunoblotted as described above. The relative expression levels of wt and mutant half-molecules were evaluated by densitometry and are indicated on the figure. *B) Effect of D792N and D1454N mutations on ATP-dependent LTC<sub>4</sub> transport activity.* Membrane vesicles (2  $\mu$ g) containing wt and the D792N and D1454N mutant MRP1 half-molecules, or control  $\beta$ -Gus were assayed for ATP-dependent LTC<sub>4</sub> transport activity by incubation in transport buffer

MOL #7708

containing [ $^3\text{H}$ ]LTC<sub>4</sub> (50 nM, 0.13  $\mu\text{Ci}$ ) at 23°C for 2 min in the presence and absence of ATP (4 mM) as described. Results shown are means  $\pm$  S.D. of triplicate determinations in a single experiment. Similar results were obtained in three additional independent experiments. *C) Effect of D792N and D1454N mutations on photolabeling with 8-azido [ $\alpha$ - $^{32}\text{P}$ ] ATP.* Membrane vesicles (20  $\mu\text{g}$ ) were incubated in transport buffer containing 8-azido [ $\alpha$ - $^{32}\text{P}$ ] ATP (5  $\mu\text{M}$ ) for 5 min at 4°C. Samples were photo-cross-linked, unincorporated nucleotides were removed and membrane proteins separated by SDS-PAGE, as described. Similar results were obtained in three independent experiments. The positions of the labeled NH<sub>2</sub>- and COOH-halves of MRP1 are shown and endogenous proteins that are also labeled are indicated (E►).

**Fig. 6.** Effect of Walker B Asp mutations on vanadate induced ADP trapping and [ $^3\text{H}$ ]LTC<sub>4</sub> photolabeling in the presence and absence of nucleotide. *A) Expression levels of wt and mutant half-molecules of MRP1.* Vesicle proteins were separated by SDS-PAGE and immunoblotted as described above. The relative expression levels of wt and mutant proteins were evaluated by densitometry and are indicated in the figure. Densitometry indicated that the level of the D1454N mutant protein in the vesicle preparation used was approximately two fold higher than in control vesicles (Fig. 6A). Consequently, the MRP1 D1454 vesicle preparation was adjusted by dilution with control vesicles prior to use in photolabeling studies, as described. *B) Effect of D792N and D1454N mutations on vanadate dependent nucleotide trapping.* Membrane vesicles (20  $\mu\text{g}$ ) were incubated for 15 min at 37°C in transport buffer containing 8-azido [ $\alpha$ - $^{32}\text{P}$ ] ATP (15  $\mu\text{M}$ ) in the absence (-) or presence (+) of 1 mM vanadate. After removal of unbound nucleotide, samples were photo-cross-linked and analyzed by SDS-PAGE. Similar results were obtained in two independent experiments. The positions of the labeled NH<sub>2</sub> - and COOH-halves of MRP1 and an

MOL #7708

endogenous protein (E►) that is also labeled are indicated. *C) Effect of D792N and D1454N mutations on LTC<sub>4</sub> photolabeling in the presence or absence of nucleotide.* Membrane vesicles (50 µg total protein) containing wt and the D792N and D1454N mutant MRP1 half-molecules were incubated in transport buffer at 23°C for 20 min in the absence or presence of ATP-γ-S (4 mM), or ATP (1 mM) plus vanadate (1 mM), prior to addition of [<sup>3</sup>H]LTC<sub>4</sub> (200 nM, 0.13 µCi). [<sup>3</sup>H]LTC<sub>4</sub> photolabeling was performed as described. Similar results were obtained in 4 additional independent experiments.

**Fig. 7.** Effect of mutating the conserved Gly residue in the signature motif on ATP-dependent transport activity, nucleotide binding, and vanadate dependent ADP trapping. *A) Expression levels of wt and G771A and G1433A mutant MRP1 half-molecules.* Vesicle proteins were separated by SDS-PAGE and immunoblotted, as described above. The relative expression levels of wt and mutant proteins were evaluated by densitometry and are indicated in the figure. *B) Effect of G771A and G1433A mutations on ATP-dependent LTC<sub>4</sub> transport activity.* Membrane vesicles (2 µg) containing wt and the G771A and G1433A mutant MRP1 half-molecules, or control β-Gus were assayed for ATP-dependent LTC<sub>4</sub> transport activity by incubation in transport buffer containing [<sup>3</sup>H]LTC<sub>4</sub> (50 nM, 0.13 µCi) at 23°C for 2 min in the presence and absence of ATP (4 mM), as described. Results shown are means ± S.D. of triplicate determinations in a single experiment. Similar results were obtained in three additional independent experiments. *C) Effect of G771A and G1433A mutations on photolabeling with 8-azido [ $\gamma$ -<sup>32</sup>P] ATP.* Membrane vesicles (20 µg) were incubated in transport buffer containing 8-azido [ $\gamma$ -<sup>32</sup>P] ATP (5 µM) for 5 min at 4°C. Samples were photo-cross-linked, unincorporated nucleotides were removed and membrane proteins separated by SDS-PAGE as described. Similar results were obtained in three

MOL #7708

independent experiments. The positions of the labeled NH<sub>2</sub>- and COOH-halves of MRP1 are shown and endogenous proteins that are also labeled are indicated (E►). *D) Effect of G771A and G1433A mutations on vanadate dependent nucleotide trapping.* Membrane vesicles (20 µg) were incubated for 15 min at 37°C in transport buffer containing 8-azido [ $\alpha$ -<sup>32</sup>P] ATP (15 µM) in the absence (-) or presence (+) of 1 mM vanadate. After removal of unbound nucleotide, samples were photo-cross-linked and analyzed by SDS-PAGE. Similar results were obtained in two independent experiments. The positions of the labeled NH<sub>2</sub>- and COOH-halves of MRP1 and that of an endogenous protein that is also labeled are indicated (E►).

**Fig. 8.** Effect of signature Gly mutations on [<sup>3</sup>H]LTC<sub>4</sub> photolabeling in the presence and absence of nucleotide. Membrane vesicles (50 µg total protein) containing wt and the *G771A* and *G1433A* mutant MRP1 half-molecules were incubated in transport buffer at 23°C for 20 min in the absence or presence of ATP-γ-S (4 mM), or ATP (1 mM) plus vanadate (1 mM), prior to addition of [<sup>3</sup>H]LTC<sub>4</sub> (200 nM, 0.13 µCi). [<sup>3</sup>H]LTC<sub>4</sub> photolabeling was performed as described. Similar results were obtained in four additional independent experiments.



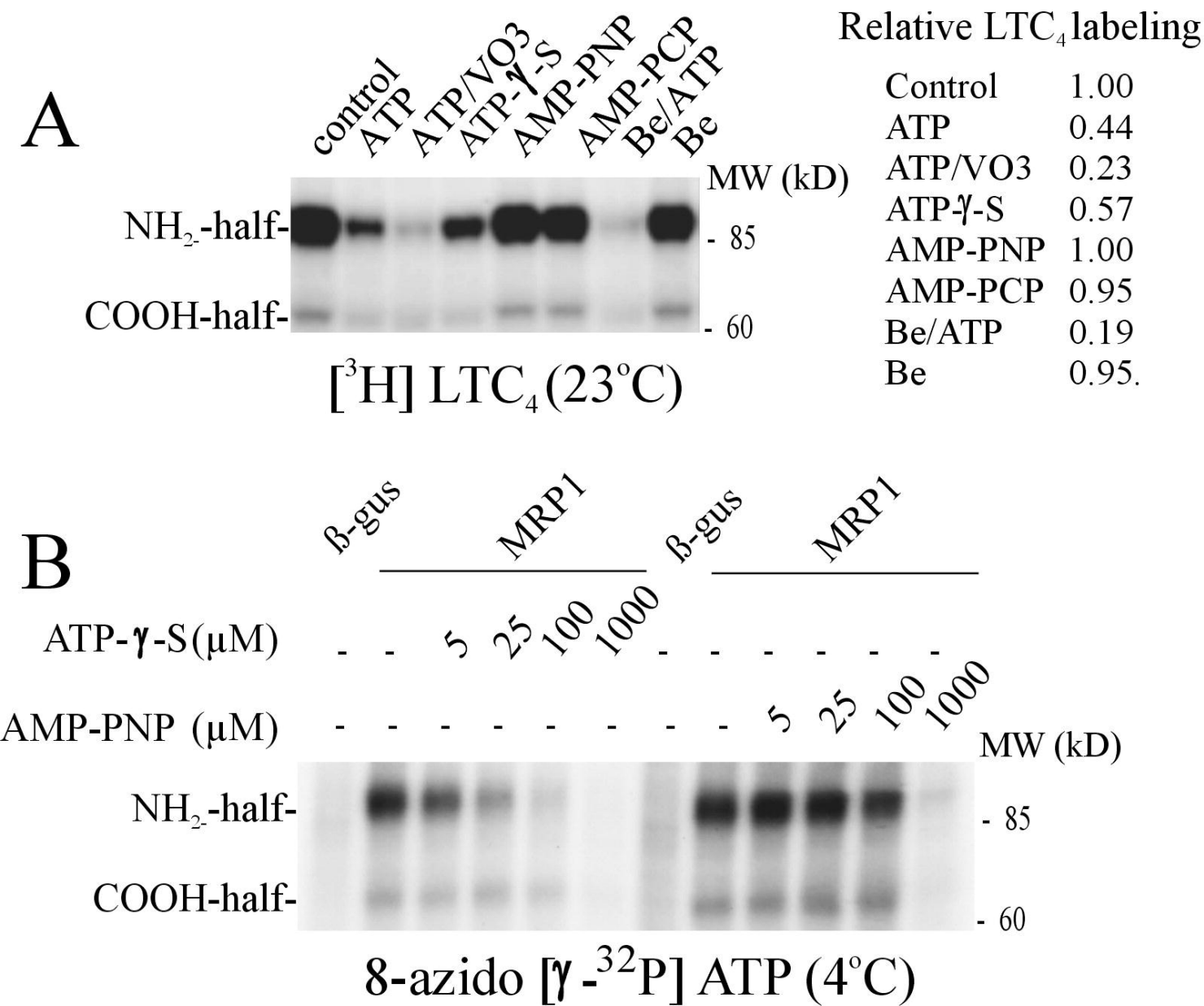


Figure 1

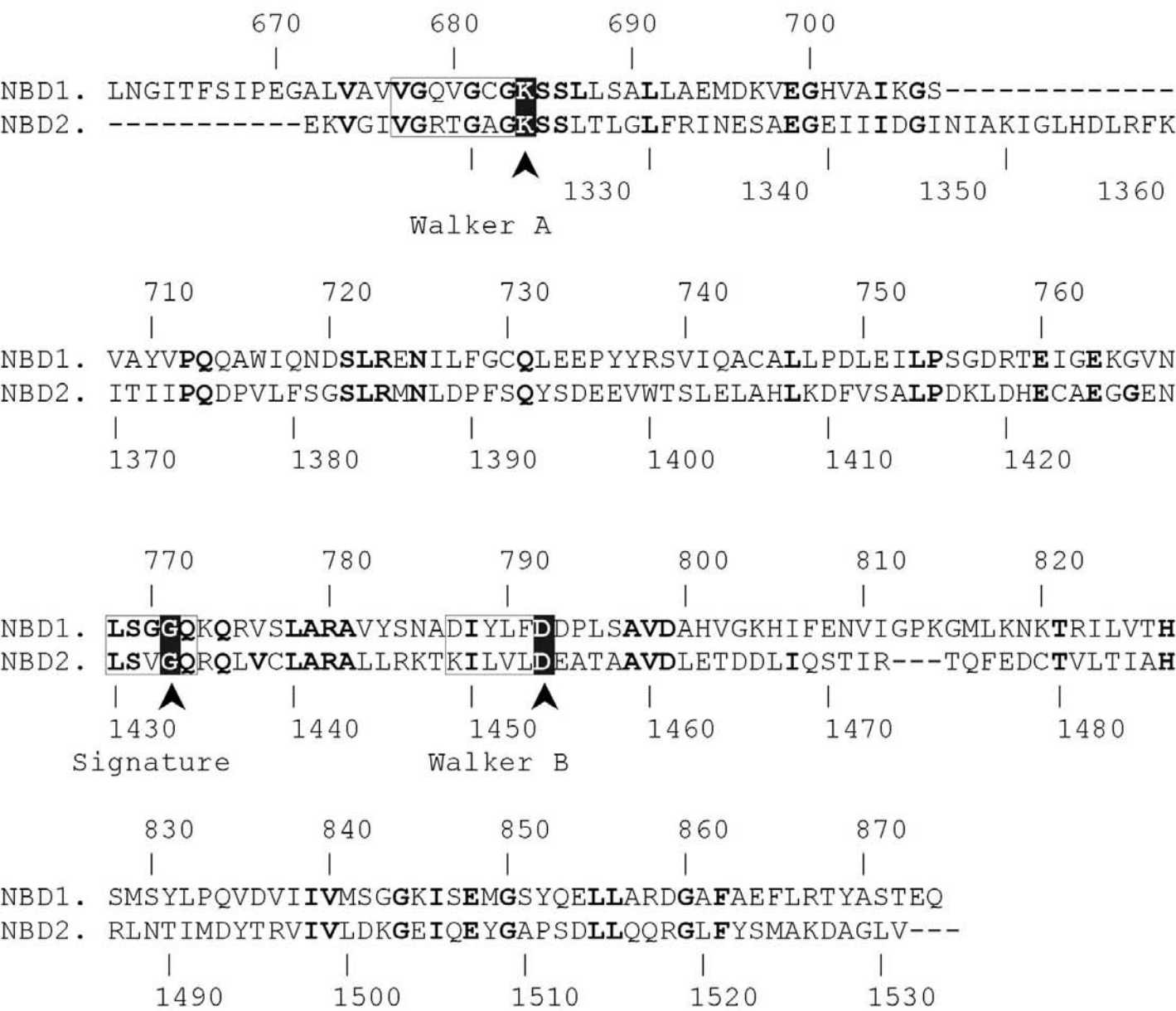


Figure 2

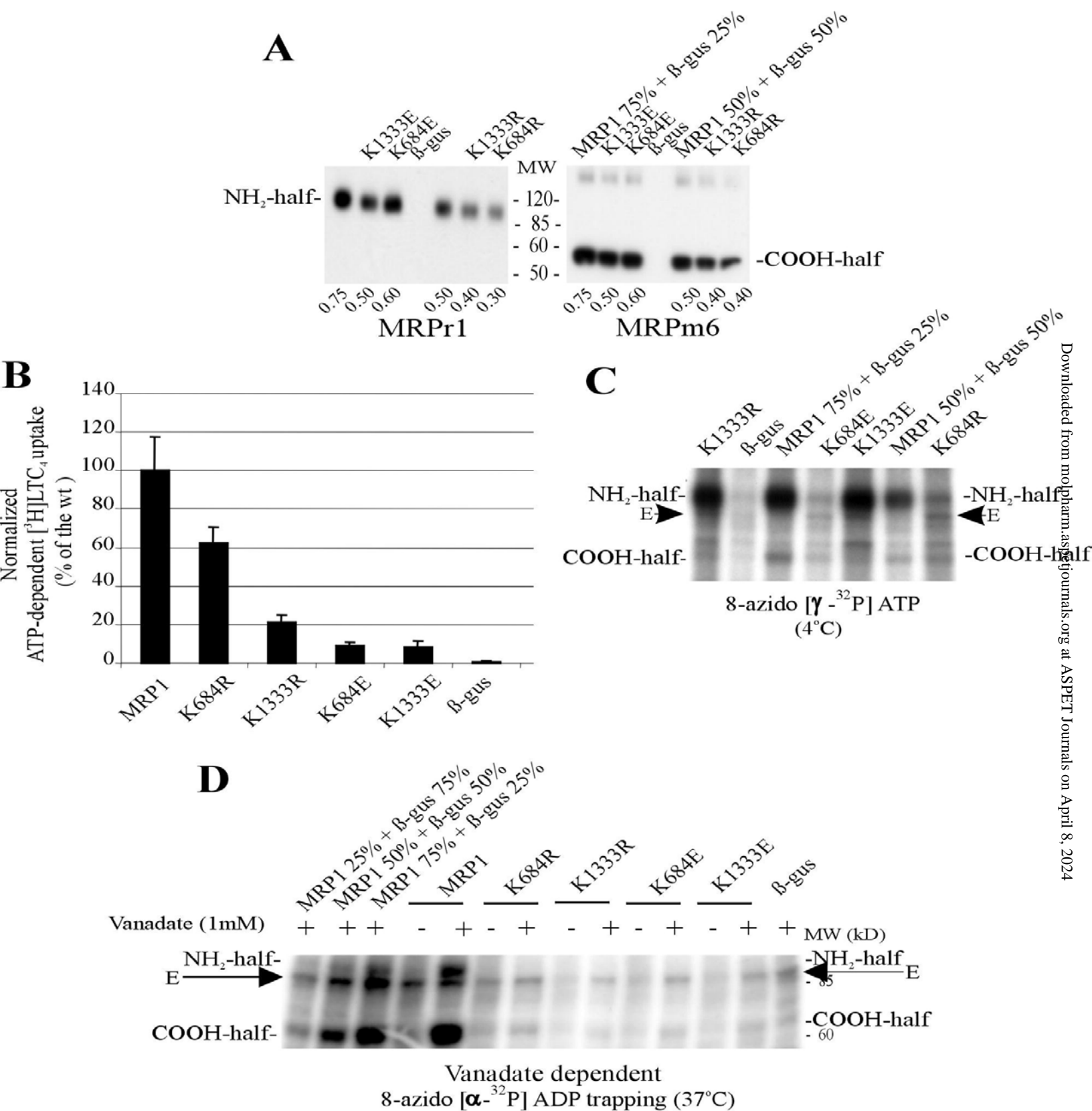


Figure 3

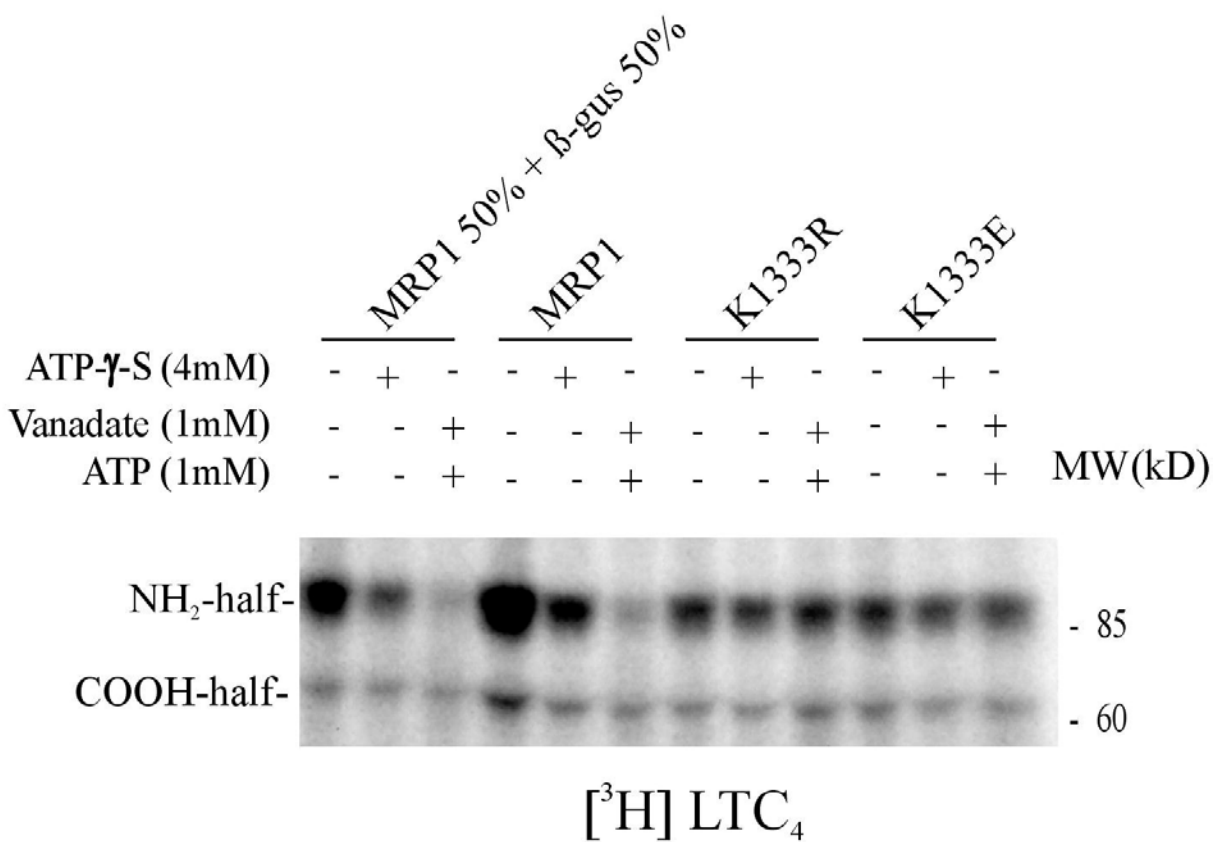
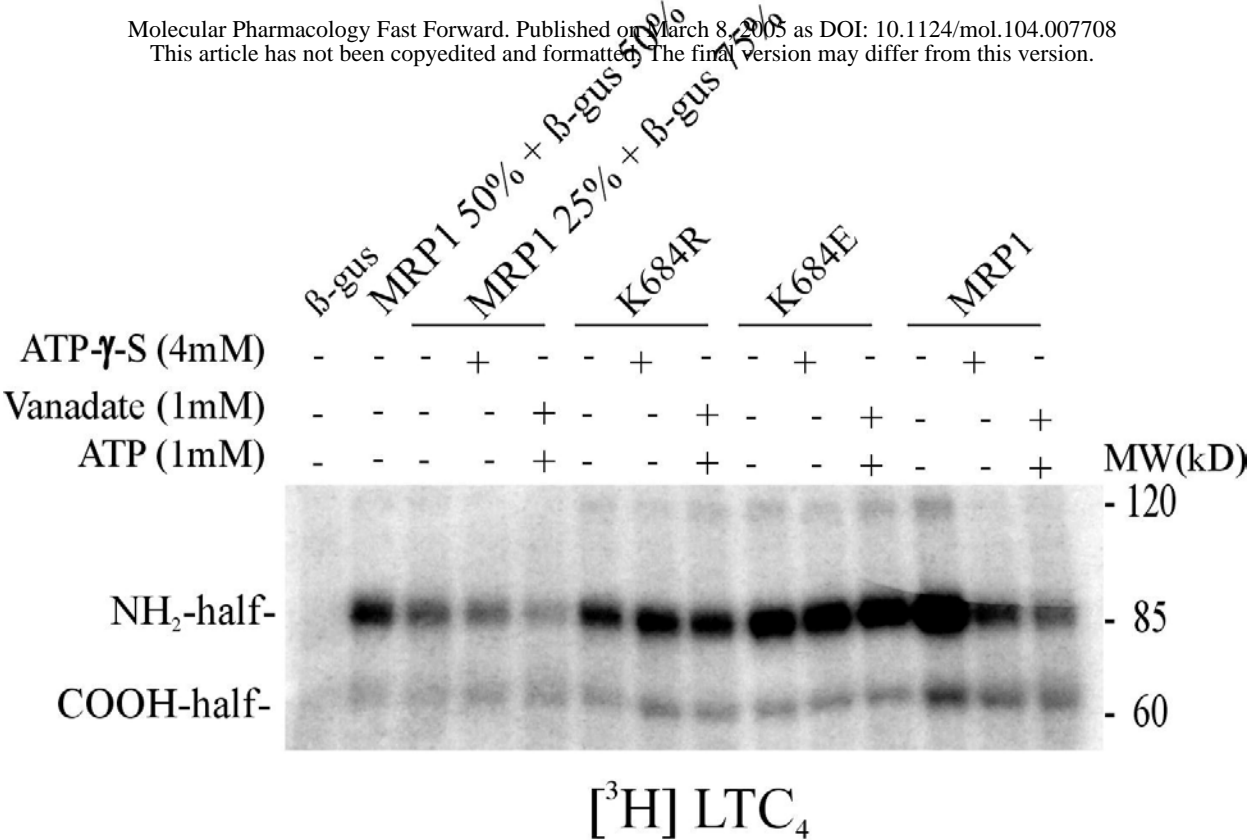


Figure 4

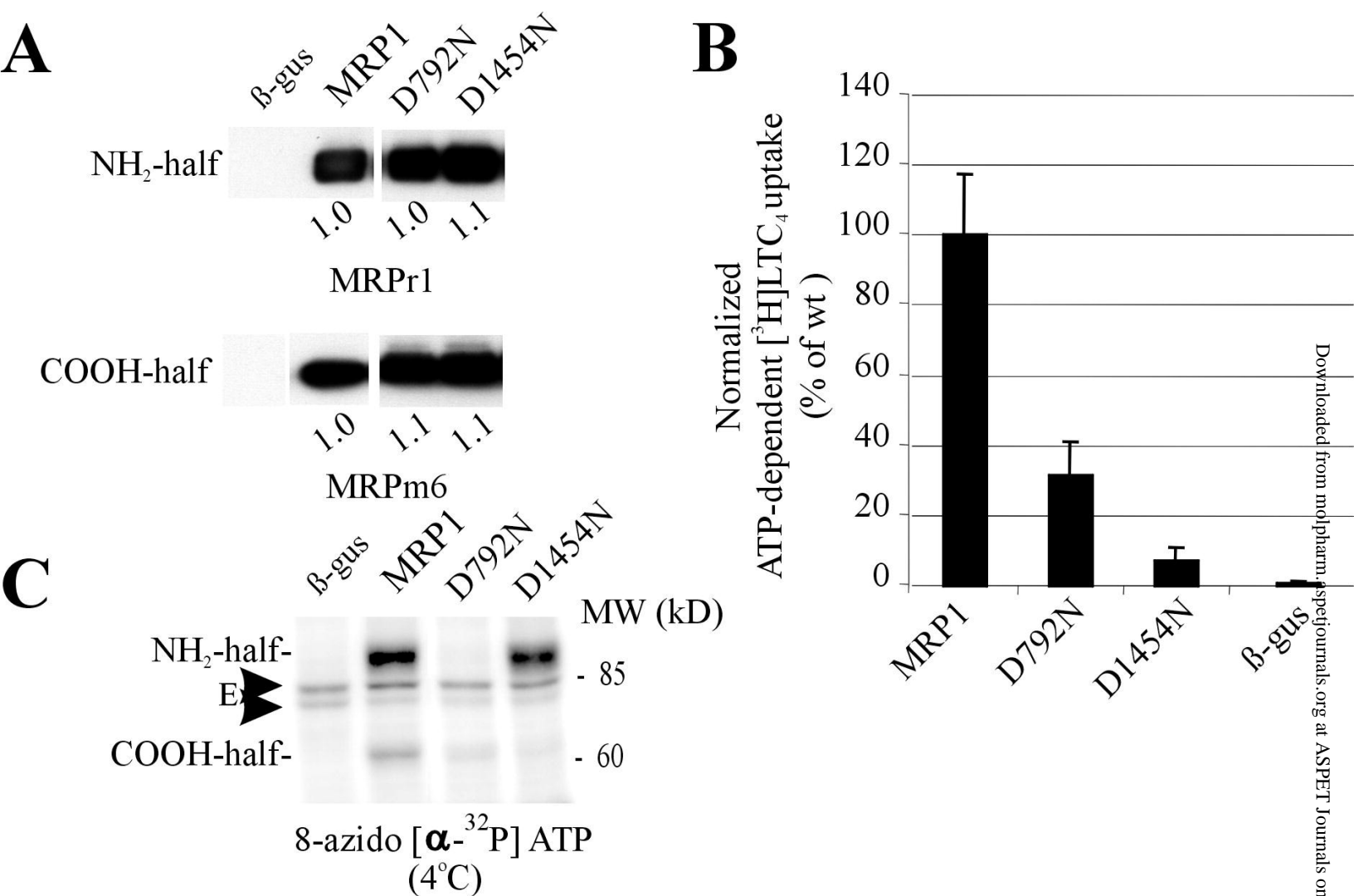


Figure 5

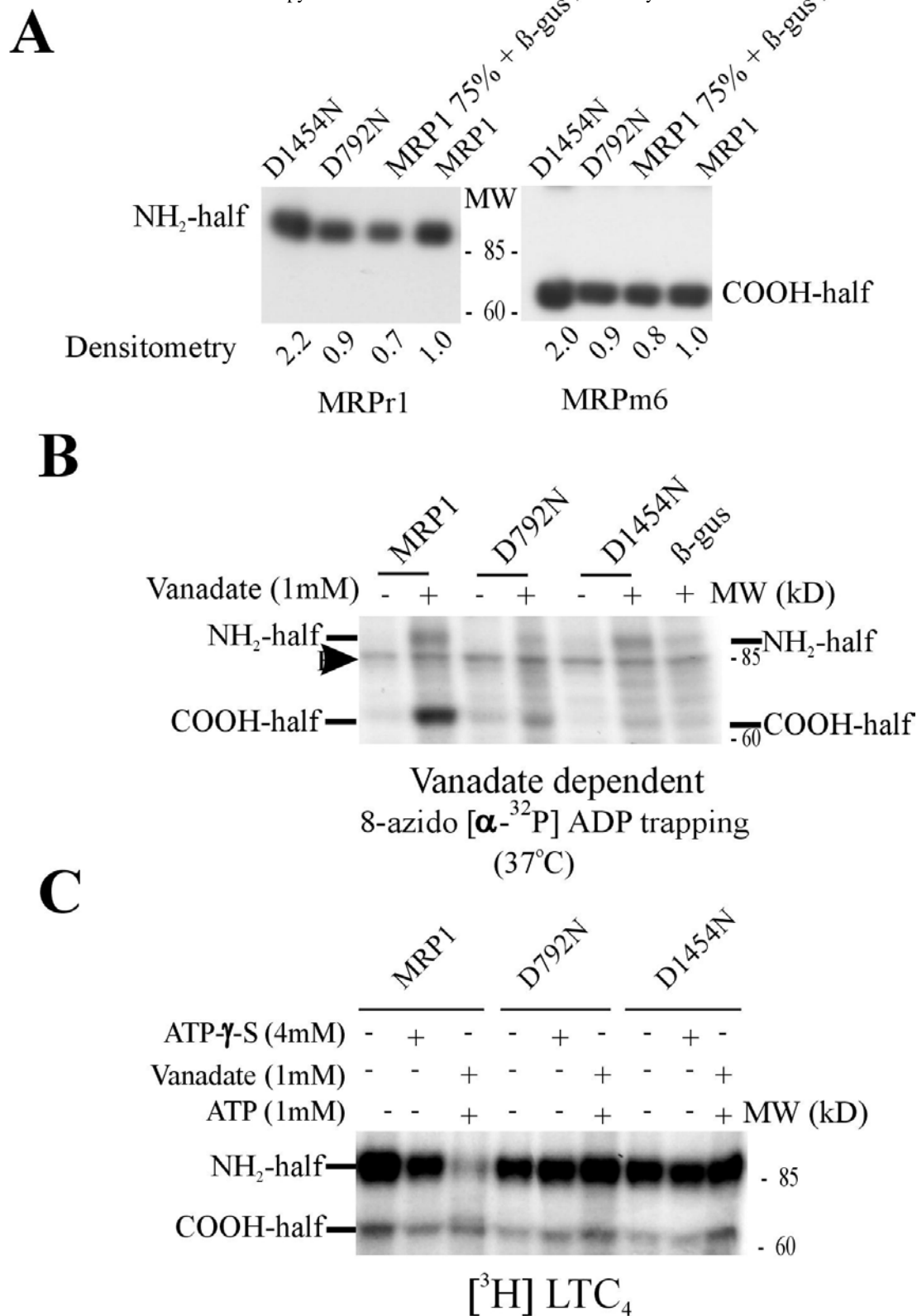


Figure 6



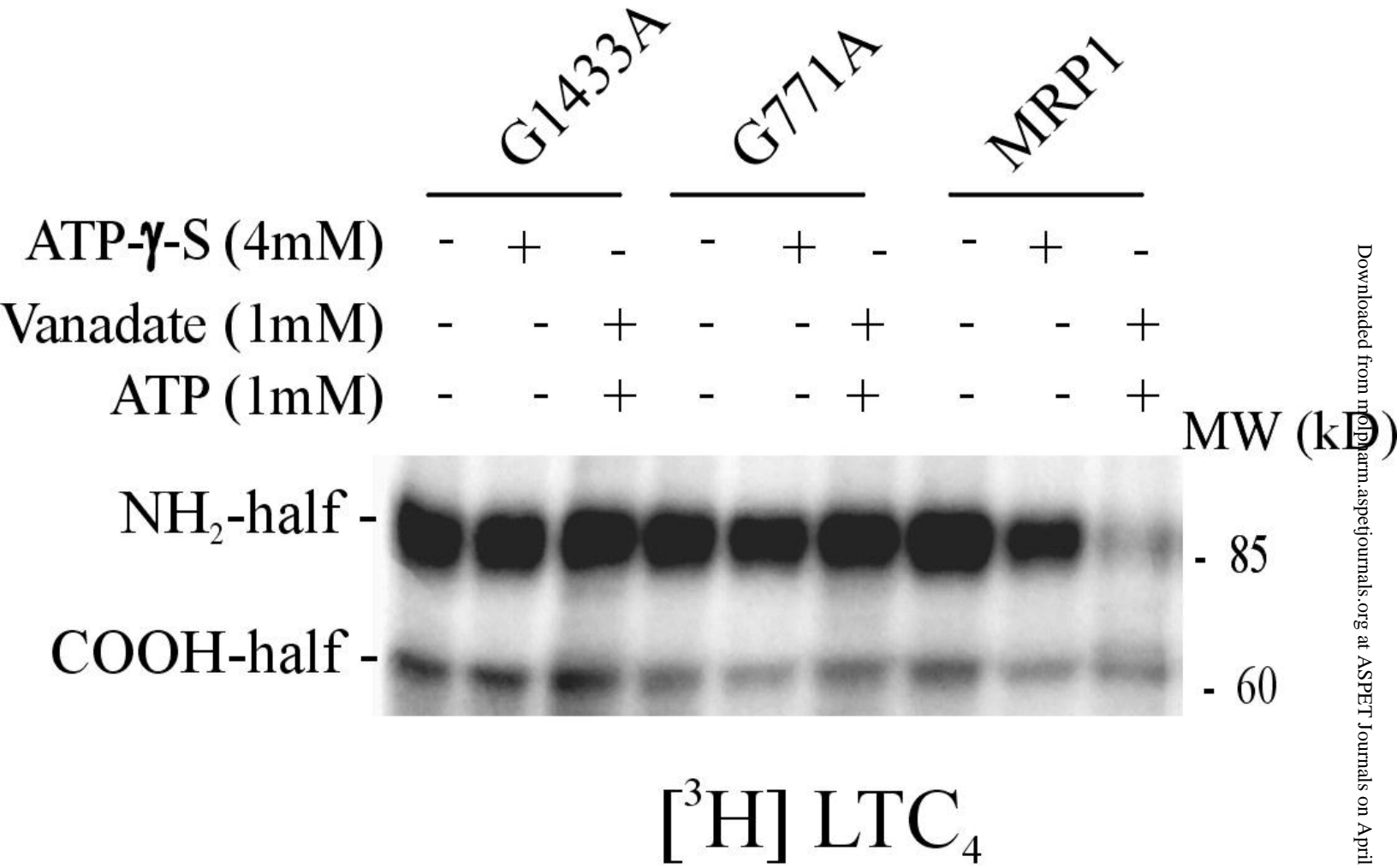


Figure 8